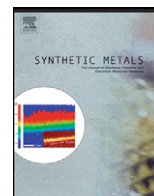




Contents lists available at ScienceDirect

## Synthetic Metals

journal homepage: [www.elsevier.com/locate/synmet](http://www.elsevier.com/locate/synmet)

# Morphology and properties of polypyrrole electro synthesized onto iron from a surfactant solution

I.L. Lehr, S.B. Saidman\*

Q1 Instituto de Ingeniería Electroquímica y Corrosión (INIEC), Departamento de Ingeniería Química, Universidad Nacional del Sur, Av. Alem 1253, 8000-Bahía Blanca-República Argentina

## ARTICLE INFO

## Article history:

Received 1 July 2008

Received in revised form 16 February 2009

Accepted 13 April 2009

Available online xxx

## Keywords:

Polypyrrole

AOT

Electrochemical polymerization

Iron electrode

Scanning electron microscopy

## ABSTRACT

The morphology of polypyrrole (PPy) deposits during electro synthesis onto iron electrodes in sodium bis(2-ethylhexyl) sulfosuccinate (AOT) solutions have been investigated using Scanning Electron Microscopy (SEM). At the early stages of electro synthesis, fibrillar, toroidal and globular forms are observed while polymerization at longer times leads to a closely packed deposit. The effects of electropolymerization parameters on the obtained morphology are discussed. It is proposed that electropolymerization rate and polymer stiffness are important factors in controlling the morphology. Electrochemical investigations demonstrate that toroid-shaped deposits present electrochemical activity. The experimental results indicate that a gelatinous product, formed as a result of iron dissolution, grows simultaneously with PPy.

© 2009 Elsevier B.V. All rights reserved.

## 1. Introduction

The chemical and electrochemical synthesis of conducting polymers continues to receive great attention in fundamental as well as in applied studies. In particular, micro- and nanostructures of polypyrrole are under active investigation because of the many existing and new possibilities for applications in optical, electrical and sensing devices [1-8]. The formation of these structures on oxidisable metals has received less attention [9,10], in spite of the obvious economical advantage.

There has also been an increasing interest in the use of conducting polymers as anti-corrosion coatings. However, the electropolymerization on oxidisable metals is difficult because the metallic electrode undergoes strong dissolution before the oxidation potential of the monomer is reached or because the development of a very protective oxide layer. Previous works have shown that stable and homogeneous PPy coatings can be deposited onto Al [11] and onto Fe [12] in the presence of sodium bis(2-ethylhexyl) sulfosuccinate (AOT) in a wide pH interval. AOT is an anionic surfactant having two bulky hydrocarbon tails and a sulfonate group in its polar head. It was postulated that pyrrole is solubilised in the micellar assembly formed on the substrate leading to highly concentrated monomer.

There is no iron dissolution before the electropolymerization starts because the formation of a protective iron oxide at pH val-

ues between 7 and 12 [12]. The electro synthesized films provide a high degree of protection against corrosion because AOT acts as an immobilized dopant.

The chemical synthesis of PPy was performed in the presence of AOT where the surfactant acts as a co-dopant together with the anion of the oxidising agent [13,14]. In contrast, the electrochemical synthesis allows to incorporate AOT as the unique dopant. The electrodeposition of PPy onto stainless steel in organic media containing AOT for the construction of a single-layer actuator has also been reported [15].

While studying this electropolymerization process onto iron electrodes it was observed the unusual formation of a gel-like product surrounding the polymer. The development of this type of structure has not been described for other electrochemical systems. EIS has been applied to characterize this system [16]. It was proposed that iron ions diffuse through the pores of the polymer and through the gel-like film developed between the polymer and the electrolyte. Finally the ions reach the gel/solution interface where they react with AOT, thickening the gel film. The gel material inside the pores inhibits the diffusion of species, contributing to difficult the corrosion of iron in chloride solutions.

The formation of the gel-like product surrounding the polymer film motivated us to study the electrochemical behaviour of iron in pure aqueous AOT solutions [17]. We found that the gelatinous material is formed onto the bare electrode as a result of iron dissolution. It was postulated that this material is a mixed NaAOT-Fe(AOT)<sub>3</sub> lamellar mesophase where the iron ion is surrounded by three AOT molecules and this structure is covered by NaAOT. The iron salt acts as a germ to produce the aggregation of AOT molecules and the

\* Corresponding author. Tel.: +54 291 4595182; fax: +54 291 4595182.  
E-mail address: [ssaidman@criba.edu.ar](mailto:ssaidman@criba.edu.ar) (S.B. Saidman).

73 birth of the layer occurs when the mesophase precipitates onto the  
74 electrode surface.

75 In this report, the investigation was extended by analysing  
76 the first stages of PPy electroynthesis in AOT solution onto iron  
77 electrodes. Different PPy morphologies were formed, which were  
78 characterized by varying electroynthesis parameters (concentra-  
79 tions of monomer and electrolyte, electropolymerization time,  
80 applied potential and temperature). We also desire to provide a  
81 deeper insight into the simultaneous formation of PPy and a gel-  
82 like product and the conditions under which these materials can  
83 be formed.

## 84 2. Experimental

85 Electrodes were prepared from pure iron rod samples. The  
86 rods were embedded in a Teflon holder with an exposed area of  
87 0.070 cm<sup>2</sup>. Before each experiment, the exposed surfaces were pol-  
88 ished to a 1000 grit finish using SiC, then degreased with acetone  
89 and washed with triply distilled water. Following this pretreatment,  
90 the electrode was immediately transferred to the electrochemi-  
91 cal cell. After polarisation, the samples were carefully and rapidly  
92 cleaned in water to avoid material losses.

93 All the potentials were measured against a saturated calomel  
94 electrode (SCE) and a platinum sheet was used as a counter  
95 electrode. The cell was a 20 cm<sup>3</sup> Metrohm measuring cell.  
96 Electrochemical measurements were done using a potentiostat-  
97 galvanostat PAR Model 273A. A dual stage ISI DS 130 SEM and  
98 an EDAX 9600 quantitative energy dispersive X-ray analyser were  
99 used to examine the PPy deposits. Iron and sulfur were determining  
100 using inductively coupled plasma atomic emission spectrometry  
101 (ICP-AES).

102 Measurements were performed in solutions containing pyrrole  
103 (Py) (0.01-1 M) and AOT (0.005-0.5 M) in a purified nitrogen gas

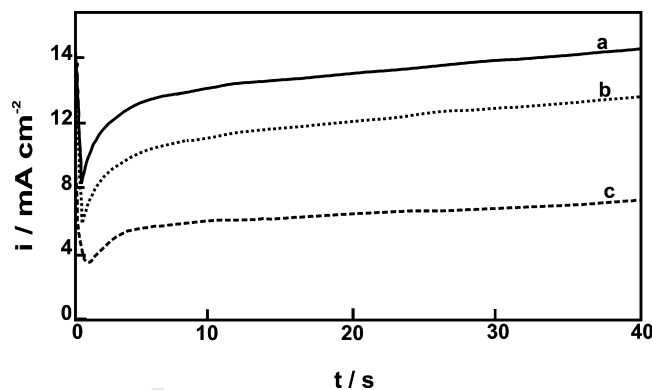


Fig. 1. Chronoamperometric curves obtained in 0.05 M AOT pH 7 containing 0.5 M Py, in response to potential steps from -1 V to: (a) 1 V, (b) 0.9 V and (c) 0.8 V.

104 saturated atmosphere at 20 °C, unless otherwise stated. The pH of  
105 the solution was adjusted by addition of NaOH. In order to avoid  
106 the slow hydrolysis of AOT all the measurements were done with  
107 freshly prepared samples. All chemicals were reagent grade and  
108 solutions were made in twice distilled water. Pyrrole was purchased  
109 from Acros Organics and it was freshly distilled under reduced pres-  
110 sure before use.

## 111 3. Results

112 The electroynthesis of PPy onto iron electrodes was done under  
113 potentiostatic control. A series of chronoamperometric curves  
114 obtained in 0.05 M AOT, pH 7, at different potential values is pre-  
115 sented in Fig. 1. The initial current decrease is associated with oxide  
116 growth and, after this stage, the formation of SEM of the polymer starts.  
117 The formed films were investigated by SEM measurements.

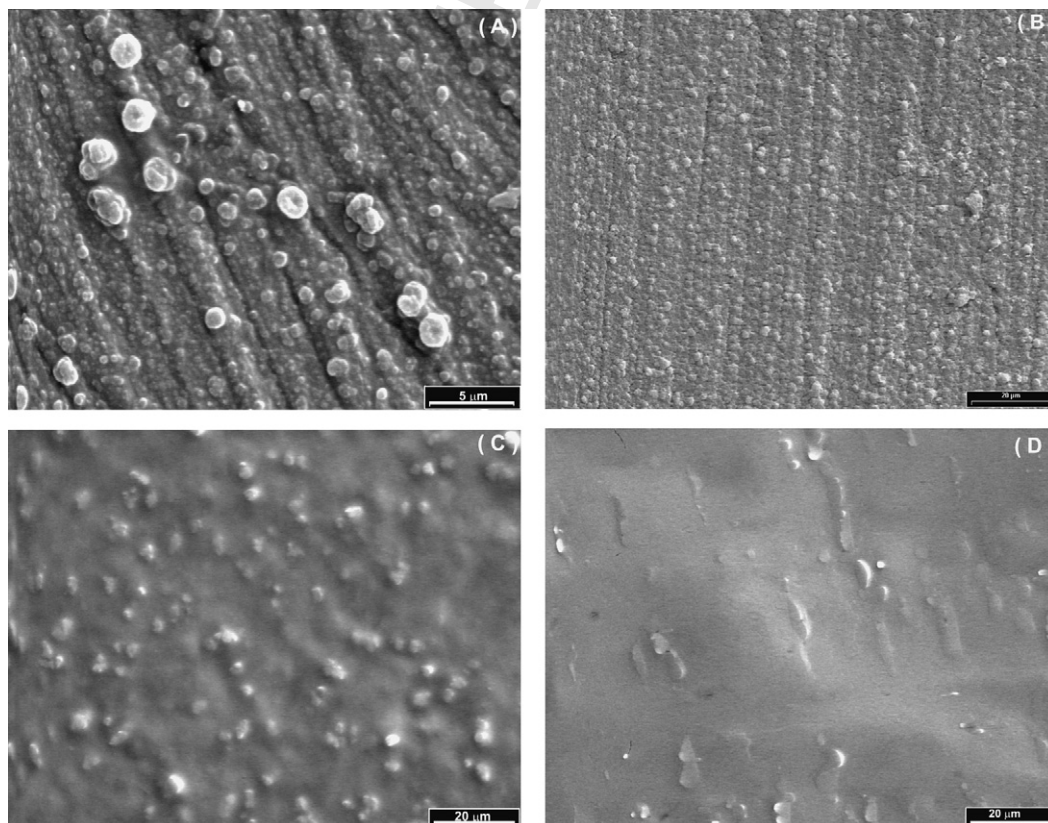
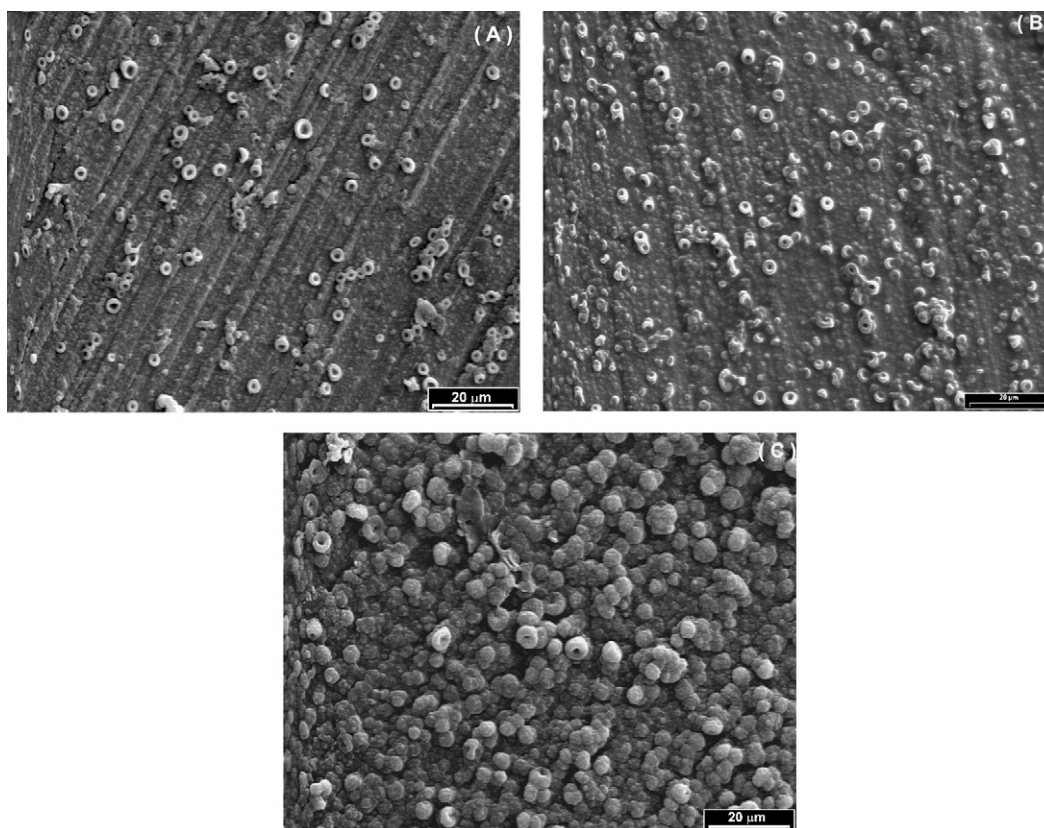


Fig. 2. SEM images of the PPy electrothesized in 0.05 M AOT, pH 7 with 0.5 M Py. The film was formed at 0.9 V for: (A) 8 s, (B) 20 s, (C) 120 s and (D) 1800 s.





**Fig. 3.** SEM images of the PPy electrosynthesized in 0.05 M AOT pH 7 with 0.5 M Py. The film was formed at 0.8 V for: (A) 8 s, (B) 20 s and (C) 40 s.

2 shows the images of PPy after different times of potentiostatic polarisation at 0.9 V. At 8 s deposition two distinctive morphologies are observed on the surface (Fig. 2A). The PPy appears to be composed of small grains with sizes around 0.5 μm homogeneously distributed on the whole iron surface. Some of these deposits seem to be toroids filled with the polymer. On top of these grains some toroidal deposits can be observed. After 20 s of deposition the whole surface is fully covered by the characteristic aggregates of microspheroidal grains (Fig. 2B). When the polarisation time is increased to 120 s, the SEM micrograph still shows the presence of the polymer but in this case underneath a smooth material (Fig. 2C). Finally, as the reaction time is further increased it can be clearly seen that this material completely covered the deposited polymer (Fig. 2D). A gelatinous product formed on top of the polymer is perceptible to the naked eye after approximately 15 min of polarisation. This product, which is also observable under galvanostatic or potentiodynamic polarisation, remains attached to the electrode when the sample is taken away from the cell.

In an attempt to gain deeper insight on the growth of the toroidal structures at the beginning of electropolymerization, a study was done by applying a lower potential to slow down the deposition rate. Fig. 3 shows images of PPy deposits during 8, 20 and 40 s of potentiostatic polarisation at 0.8 V. Toroids can be observed on top of a granular deposit (Fig. 3A). These structures do not differ very much in size, having an outer diameter of about 2 μm. A longer deposition time results in a larger number of toroids and it would seem that they grow from the grains previously formed (Fig. 3B). The majority of them are oriented parallel to the electrode surface. It can be also observed that some of them are packed together to form three-dimensional agglomerates. In comparison with the electrodeposition at 0.9 V, polarisation at 0.8 V leads to an increased number of toroidal structures which possess a smoother texture. As the polymerization proceeds further, the hole of toroids

is sealed by additional growth and they are no longer distinguished as individual entities in the midst of the grained film (Fig. 3C).

When the film was electropolymerized at 0.7 V the proportion of toroid-like deposits is smaller and several of them are incomplete toroids (Fig. 4). The formation of the characteristic grains of PPy is favoured when the electropolymerization potential was raised to 1 V.

We did not observe toroidal PPy deposits in the presence of SDBS (sodium dodecylbenzene sulfonate) instead AOT under the same experimental conditions detailed above. In this case, only the deposition of the usual grained structure occurred. Likewise, the morphological characteristics of the polymer also depend

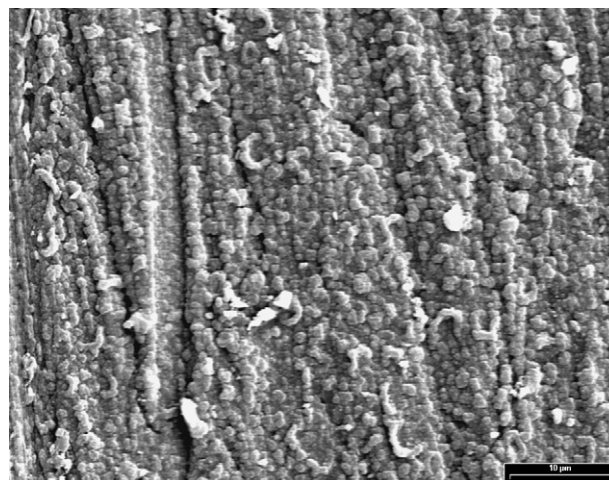


**Fig. 4.** SEM image of the PPy electrosynthesized in 0.05 M AOT pH 7 with 0.5 M Py. The film was formed at 0.7 V for 20 s.

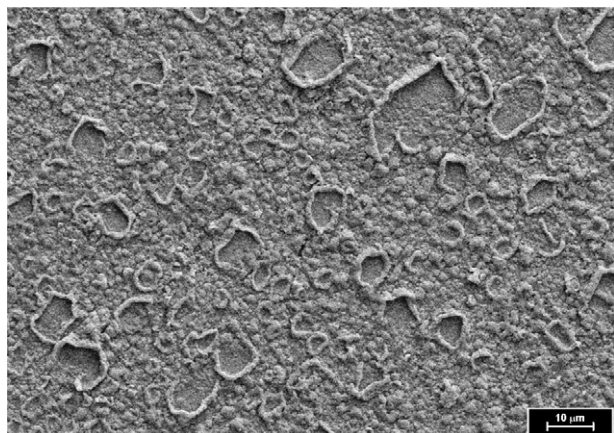


Fig. 5. SEM image of the PPY electrosynthesized in 0.005 M AOT pH 7 with 0.5 M Py. The film was formed at 0.8 V for 80 s.

on the electrochemical polymerization conditions. Galvanostatic electrodeposition but consuming the same charge than that corresponding to potentiostatic polarisation, leads only to the usual PPY morphology.

When the surfactant concentration was lowered to 0.005 M, small globules and toroids were observed coexisting with a lot quantity of bigger near-circular structures (Fig. 5). Electrodeposition was done at 0.8 V with the same charge used for electroynthesis in 0.05 M AOT during 20 s. The big structures are about three times larger than toroids observed at higher AOT concentration and they are similar to ones reported by other authors [3,5], although here their shapes are less circular. It can be also observed worm-like fibrillar morphologies which grew parallel to the electrode surface. It appears that a great amount of large worm-like deposits grow until they enclosed themselves into more or less circular morphologies. An increase in AOT concentration to 0.5 M promotes the formation of the gelatinous material even at low electropolymerization times. PPY deposits obtained under this condition have globular morphology.

Decreasing the monomer concentration to 0.05 M resulted in a thicker gel-like product and a rare observation of toroids could be made. When the concentration of Py was increased up to 1 M, toroids similar to that previously described were obtained, although their mean diameter was higher (5 μm).

Temperature is another factor that affects electropolymerization, increasing the kinetics of the reactions. Results obtained at 5 °C indicate that the number of deposited toroids decreased with respect to that obtained at 20 °C (Fig. 6). In addition, these deposits have almost equal diameter than those formed at 20 °C, although several of them are not well-defined toroids. Electropolymerization at 60 °C yielded mainly non-toroidal morphologies and increased amounts of the gel material.

The redox switching behaviour of the electrosynthesized films was examined in monomer-free solutions (Fig. 7). The reduction scan presents only a reduction peak at very negative potentials attributable to Na<sup>+</sup> insertion into the polymer matrix [18]. The intensity of both oxidation and reduction peaks increases linearly with scan rate in the range 1–100 V s<sup>-1</sup> (Fig. 8), indicating a surface-attached redox species.

The charge obtained by the integration of the cathodic peak corresponds to 12% and 10% of the charge used for deposition of the film during 20 s at 0.8 and 0.9 V, respectively (Fig. 7, curves (a) and (b)). The values do not differ markedly in spite of the differences in polymer morphology (toroids and grained deposits). This result is consistent with an active surface area of the doughnut-like deposits exposed to the solution. As was stated, galvanostatic con-

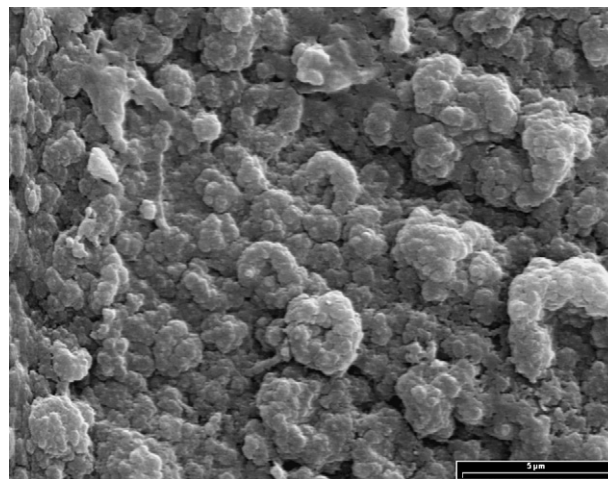


Fig. 6. SEM images of the PPY electrosynthesized in 0.05 M AOT pH 7 with 0.5 M Py. The film was formed at 0.8 V for 20 s at 5 °C.

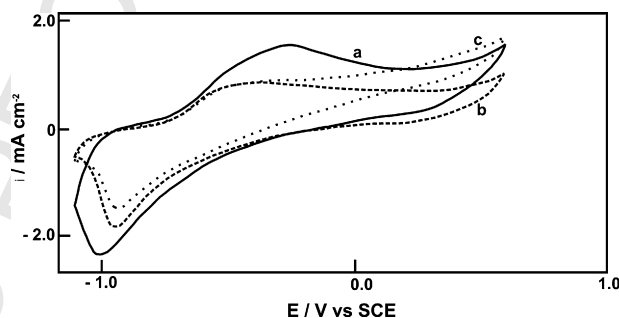


Fig. 7. Cyclic voltammograms of PPY-coated iron electrode at 0.05 V s<sup>-1</sup> in 0.05 M AOT pH 7. The PPY films were made in the same solutions containing 0.5 M Py at: (a) 0.9 V, 20 s; (b) 0.8 V, 20 s; and (c)  $i = 5 \text{ mA cm}^{-2}$ , 28 s. The fifth cycle is displayed. Initial potential: 0.6 V.

ditions leads to a morphology resembling that obtained when the electrode is polarised at 0.9 V. The integrated reduction charge is in this case 9% of the charge consumed during deposition (Fig. 7, curve (c)), a value that does not differ significantly from the previous ones. In addition, the redox switching behaviour of the PPY films is practically independent of electropolymerization temperature in the range between 5 and 60 °C, even though the morphology varies with temperature.

Further details can be obtained from EDX analysis of the electro-synthesized films shown in Fig. 2. The signal of iron progressively

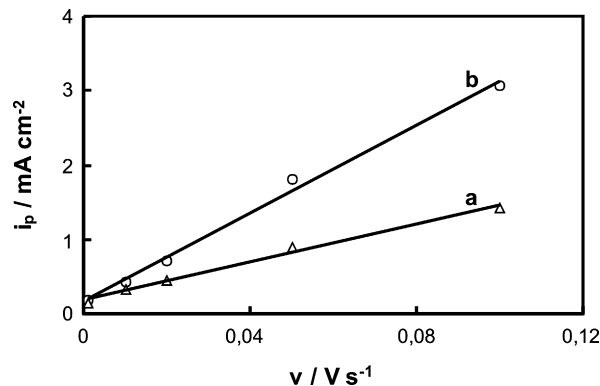
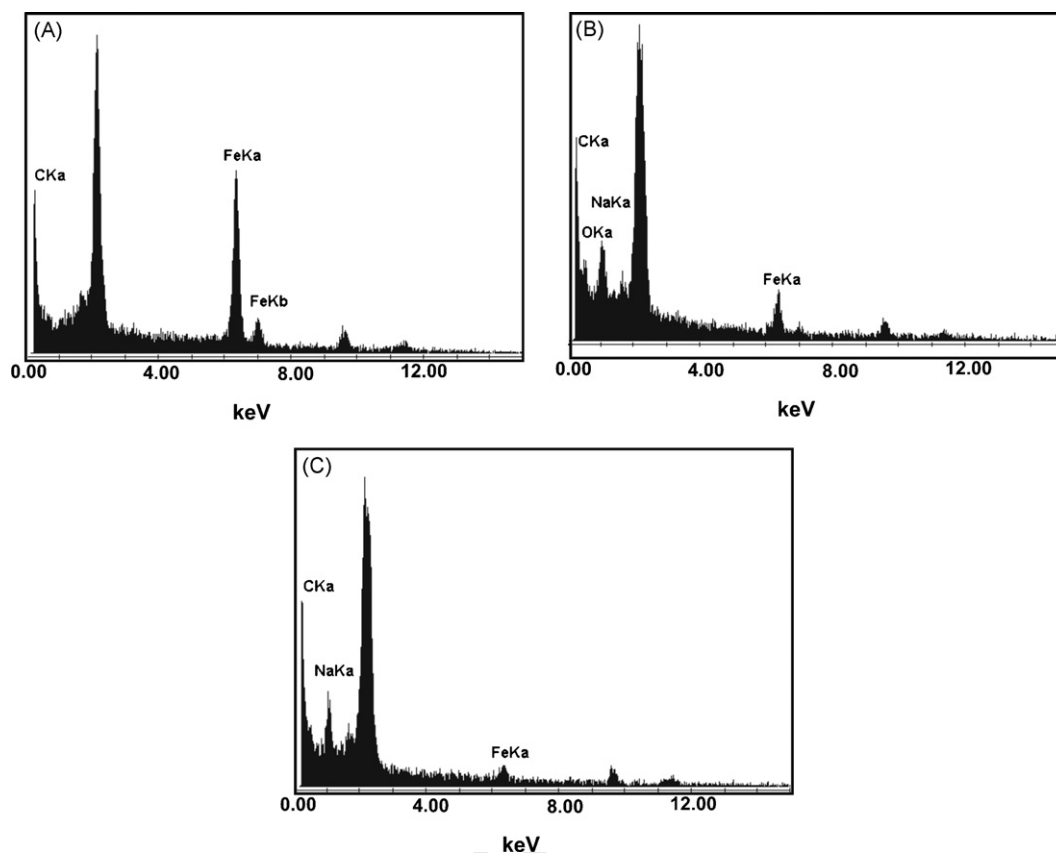


Fig. 8. Dependence of peak current ( $i_p$ ) on the scan rate ( $\nu$ ) for a PPY-coated iron electrode in 0.05 M AOT, pH 7. The PPY film was made in the same solution containing 0.5 M Py at 0.8 V for 20 s. (a) Anodic and (b) cathodic.





**Fig. 9.** EDX examination of PPy-coated iron. The film was formed at 0.9 V in 0.05 M AOT, pH 7 solution containing 0.5 M Py at: (A) 20 s, (B) 120 s and (C) 1800 s.

decreases with the electropolymerization time, indicating the thickening of a homogeneous deposit (Fig. 9). Moreover, this result suggests that oxidised iron is not concentrated in the gelling material in contact with the electrolyte solution. Compared with the signal that comes only from the polymer (Fig. 9A), the EDX analysis shows an increasing amount of Na when the gel is sufficiently developed to cover the polymer (Fig. 9C), corroborating that the lamellar mesophase contains NaAOT.

A portion of the gel formed simultaneously with the polymer was carefully removed from the electrode and its analysis indicates a content of iron of 0.2%. Because the lamellar structure can be growth as long as there is sufficient  $\text{Fe}(\text{AOT})_3$ , the release of a small amount of dissolved iron in the boundary between the polymer and the gel assures further growth of the gel. The Fe/S molar ratio found in the gel was 5.0, corroborating that the  $\text{Fe}(\text{AOT})_3$  is covered by NaAOT. A higher value, 7.5, was determined when no PPy was formed [17], indicating that a lower amount of NaAOT is incorporated into the lamellar organization that grows on top of the PPy.

#### 4. Discussion

A variety of interesting electrosynthesized PPy microstructures such as plates, bowls and cups has been described. The growth process was explained by a self-assembled gas bubble template mechanism, where the bubbles correspond to hydrogen gas released from the counter electrode or oxygen gas produced on the working electrode [1,9,19,20]. Toroid-shaped morphology does not seem to be the result of this kind of growth mechanism.

It has also been proposed that microstructures can be electrochemically synthesized with self-assembled surfactants onto the electrode surface as the templates [6,21,22]. It is difficult to estimate

whether the formation of toroidal deposits is a result of the kind of surfactant since this type of structures has also been obtained from other electrolytes but using non-oxidisable substrates. Fujikawa et al. were the first in reporting the formation of toroid-shaped PPy structures, which were deposited from sodium perchlorate aqueous solution [3]. Later this type of morphology was obtained for PPy electrodeposition from tetrabutylammonium perchlorate in acetonitrile [5] and more recently for PPy electrodeposition in nitrate solution [23].

The chemical synthesis with the addition of AOT results in a globular morphology, although it should be taken into account that in this case AOT acts as a co-dopant [13,14]. The potentiostatic synthesis of PPy onto stainless steel in organic media also results in a globular morphology [15].

The synthesis of nanomaterials like metal oxides, salts or peptides, among others, with toroid-shaped morphology has been reported [24–26]. But the formation of DNA toroids is undoubtedly the most studied. It is well demonstrated that DNA in solution can be made to condense with the addition of several chemical agents and that condensation often results in a toroidal structure. In spite of toroid organization during DNA has been investigated for decades there is no accordance about the exact reasons for the formation of this type of morphology [27–30].

Our results demonstrate that a wide distribution of PPy structures was obtained under the different experimental conditions. However, it is possible to conclude that the majority of the formed structures are complete and thick toroids at defined electropolymerization rates. The formation of PPy granules is enhanced by increasing the deposition rate while the formation of near-circular structures such as that presented in Fig. 3 is promoted at lower rates. Considering the experimental conditions in this work, high values of monomer and dopant concentrations as well as of temperature

and applied potential accelerate deposition rate. It should be mentioned that all the structures grew onto an underlying PPy film of granular morphology, in accordance to that found for the formation of tubular PPy structures [9,10].

But the electropolymerization rate is probably not the unique factor that controls the morphology. Chain stiffness is an important parameter that conditions the geometry in the case of DNA condensates [28,29]. Low stiffness results in a globular morphology and as this parameter is increased, loops tend to clump together and wind about a common axis to form a ring or pretorus structure [28]. Later in this paper the dependence between stiffness and dopant characteristics will be discussed.

The near-circular structures formed under low electrodeposition rates seem to initiate as worm-like fibrillar deposits that grow in a horizontal direction with respect to the substrate surface. Flexibility of the polymer chains is such that most of the worm-like structures bent forming near-circular morphologies. In studying the formation of PPy nanowires Zhang et al. have shown that some nanowires were twisted tightly and some even enclosed themselves into more or less ring-like structures [22]. The authors suggested that PPy long chains tend to entangle together due to hydrogen bonding and  $\pi$ - $\pi$  interactions among themselves.

Then, it is possible that polymer stiffness also plays an important role in controlling the morphologies described here. Stiffness depends on the dopant characteristics. Dopants with a relative large size reduce interchain interactions such as hydrogen bonding and  $\pi$ - $\pi$  interactions. This results in an increased distance between polymer backbones, causing a more flexible structure. But at the same time steric effects would make difficult the formation of completely enclosed structures.

Thus, the formation of toroids depends of the combined effects of two principal factors: electropolymerization rate and polymer flexibility. The dominant morphology changes from twisted worm-like shapes to toroids and finally to globules by increasing both parameters. The effect of dopant size cannot be easily predicted. This general picture explains the formation of PPy deposits with a great variety of shapes, and also the variety of experimental conditions for electropolymerization that produce, i.e., toroids deposition [3,5,23].

The picture is much more complicated when considering that AOT not only acts as a dopant but also as a surfactant. The phase diagram of the binary system of AOT–water indicates that an isotropic micellar phase exists for concentrations below 0.02 M, above which a lamellar phase was identified [31]. The electropolymerization rate increases in the presence of the surfactant because the monomer is preferentially dissolved in the micellar assembly due to its hydrophobic nature. It should be also taken into account that the structure of the micelles will be permanently disrupted when the surfactant serves as dopant [22].

In addition to the points described above, depending on the ratio of AOT to monomer the prevailing reaction will be the electropolymerization or the gel-like material formation. At high ratios, the developed morphology is dominated by the presence of the gel. The same occurs at high electropolymerization temperatures. The present results also demonstrate that the gel material emerges in an early stage of polymerization and that it does not hinder the PPy growth. Iron is dissolved and reacts with AOT providing sites for the formation of the lamellar mesophase. Then both, PPy and the gelatinous material grow simultaneously. The ratio of AOT to monomer will condition the relative contribution of each reaction.

The above results indicate that the PPy structures obtained during the first growth stage are electroactive and that their redox properties are independent of polymer morphology.

The formation of toroid-shaped structures onto a substrate like iron opens new possibilities to fabricate microstructured PPy with good morphological qualities. This type of deposits has the poten-

tiality of biomaterial immobilization on the surface for detection by electrochemical methods in biosensing area [3]. In addition, the doughnut-shaped drug delivery system provides an easy and effective alternative in controlling the rate of delivery for many drugs [32]. The electroactive PPy films are also expected to have applications in the construction of actuator devices. Because AOT remains entrapped into the polymer matrix during electrochemical switching only small and mobile positively charged ions such as  $\text{Na}^+$  are transported into and out of the film. This type of redox behaviour constitutes an advantage for actuator devices [33]. On the other hand, PPy doped with large anionic detergents shows a much higher chemical stability in aqueous solutions compared with the polymer doped with smaller anions [34].

## 5. Conclusions

It is proposed that two principal variables condition the morphology of PPy electrodeposited onto iron electrodes in AOT solutions. The one is the electropolymerization rate and the other is the polymer chains flexibility. An increase in both parameters promotes that morphology changes from fibrillar to toroidal, to globular. Dopants with a relative large size favour a more plasticized polymer, although they have more than one effect on the morphology.

Under defined experimental conditions electrochemically active toroids are formed. The majority of toroids are oriented parallel to the electrode surface and some of them are packed together compactly to form three-dimensional aggregates. They are filled in by additional growth and then the PPy film exhibits its usual morphology.

The formation of a gel-like material occurs simultaneously with electropolymerization. This product is a result of iron dissolution in the AOT solution. The polymer is formed first but it does not hinder the development of the gel. The development of the gel initiates into the PPy channels and it continues growing until covering the whole polymer matrix.

## Acknowledgements

CONICET, ANPCYT and Universidad Nacional del Sur, Bahía Blanca, Argentina are acknowledged for financial support.

## References

- [1] L. Qu, G. Shi, F. Chen, J. Zhang, *Macromolecules* 36 (2003) 1063.
- [2] A.D.W. Carswell, E.A. O'Rear, B.P. Grady, *J. Am. Chem. Soc.* 125 (2003) 14793.
- [3] K. Fujikawa, H.S. Jung, J.W. Park, J.M. Kim, H.Y. Lee, T. Kawai, *Electrochem. Commun.* 6 (2004) 461.
- [4] A. Wu, H. Kolla, S.K. Manohar, *Macromolecules* 38 (2005) 7873.
- [5] J. Hartung, J. Kowalik, Ch. Kranz, J. Janata, M. Josowicz, A. Sinha, K. McCoy, *J. Electrochem. Soc.* 152 (2005) E345.
- [6] M. Acik, C. Bastiran, G. Sonmez, *J. Mater. Sci.* 41 (2006) 4678.
- [7] W. Zhong, S. Liu, X. Chen, Y. Wang, W. Yang, *Macromolecules* 39 (2006) 3224.
- [8] Y. Gao, L. Zhao, H. Bai, Q. Chen, G. Shi, *J. Electroanal. Chem.* 597 (2006) 13.
- [9] G. Chen, D.E. Tallman, G.P. Bierwagen, *J. Solid State Electrochem.* 8 (2004) 505.
- [10] A. Eftekhari, M. Harati, M. Pazouki, *Synth. Met.* 156 (2006) 643.
- [11] I.L. Lehr, S.B. Saidman, *Mat. Chem. Phys.* 100 (2006) 262.
- [12] I.L. Lehr, S.B. Saidman, *Corros. Sci.* 49 (2007) 2210.
- [13] M. Omasová, M. Trchová, J. Pionteck, J. Prokeš, J. Stejskal, *Synth. Met.* 143 (2004) 153.
- [14] K. Boukerma, M. Omasová, P. Fedorko, M.M. Chehimi, *Appl. Surf. Sci.* 249 (2005) 303.
- [15] G. Han, G. Shi, *Sens. Actuators B* 113 (2006) 259.
- [16] I.L. Lehr, S.B. Saidman, *React. Fun. Polym.* 68 (2008) 1152.
- [17] I.L. Lehr, S.B. Saidman, P.C. Schulz, *J. Colloid Interface Sci.* 306 (2007) 323.
- [18] S.B. Saidman, *Electrochim. Acta* 48 (2003) 1719.
- [19] P. Lemon, J. Haigh, *Mater. Res. Bull.* 34 (1999) 665.
- [20] L. Qu, G. Shi, J. Yuan, G. Han, F. Chen, *J. Electroanal. Chem.* 561 (2004) 149.
- [21] G. Lu, C. Li, G. Shi, *Polymer* 47 (2006) 1778.
- [22] X. Zhang, J. Zhang, W. Song, Z. Liu, *J. Phys. Chem. B* 110 (2006) 1158.
- [23] E. Garfias-García, M. Romero-Romo, M.T. Ramírez-Silva, J. Morales, M. Palomar-Pardavé, *J. Electroanal. Chem.* 613 (2008) 67.

- 413 [24] A.E. Giannakas, T.C. Vaimakis, A.K. Ladavos, P.N. Trikalitis, P.J. Pomonis, J. Colloid  
414 Interface Sci. 259 (2003) 244.
- 415 [25] S. Thachepan, M. Li, S.A. Davis, S. Mann, Chem. Mater. 18 (2006) 3557.
- 416 [26] M. Diociaiuti, F. Bordi, A. Motta, A. Carosi, A. Molinari, G. Arancia, C. Coluzza,  
417 Biophys. J. 82 (2002) 3198.
- 418 [27] C.C. Conwell, N.V. Hud, Biochemistry 43 (2004) 5380.
- [28] I.R. Cooke, D.R.M. Williams, Phys. A 339 (2004) 45.
- [29] G. Maurstad, B.T. Stokke, Curr. Opin. Colloid Interface Sci. 10 (2005) 16.
- [30] I.M. Kulic, D. Andrienko, M. Deserno, Europhys. Lett. 67 (2004) 418.
- [31] P.G. Petrov, S.V. Ahir, E.M. Terentjev, Langmuir 18 (2002) 9133.
- [32] E. Sundry, M.P. Danckwerts, Eur. J. Pharm. Sci. 22 (2004) 477.
- [33] S. Shimoda, E. Smela, Electrochim. Acta 44 (1998) 219.
- [34] L. Bay, N. Mogensen, S. Skaarup, P. Sommer-Larsen, M. Jrgensen, K. West, Macro-  
molecules 35 (2002) 9345.

UNCORRECTED PROOF